

{311} defects in silicon: The source of the loops

Jinghong Li and Kevin S. Jones

Department of Materials Science and Engineering, SWAMP Center, University of Florida, Gainesville, Florida 32611-6400

(Received 28 August 1998; accepted for publication 19 October 1998)

The annealing kinetics of extended defects in Si⁺-implanted Si have been investigated by *in situ* annealing plan-view transmission electron microscopy (TEM) samples in a TEM. A $\langle 100 \rangle$ Czochralski-grown silicon wafer was implanted with 100 keV Si⁺ at the subamorphizing dose of $2 \times 10^{14} \text{ cm}^{-2}$. Following implantation, the effect of annealing of 800 °C was studied by *in situ* annealing. After 5 min of annealing at 800 °C, a dense collection of both {311} defects ($3 \times 10^{11}/\text{cm}^2$) and small subthreshold dislocation loops ($1 \times 10^{11}/\text{cm}^2$) were observed. Upon subsequent annealing, the {311} defect density decreased rapidly and the loop density increased. The evolution of approximately 500 {311} defects could be followed as a function of annealing time. The unfauling of a {311} defect was observed to be the source of every subthreshold loop observed to form (about 150 loops in the monitored region). After the initial 5 min anneal at 800 °C, the probability of a {311} unfauling into a loop was about 50%. Based on these observations, it is concluded that unfauling of the {311} defects is the source of the subthreshold dislocation loops in nonamorphized ion-implanted silicon. 70% of the loops formed were determined to have a Burgers vector of $a/3\langle 111 \rangle$, while 30% were perfect with a Burgers vector of $a/2\langle 110 \rangle$. © 1998 American Institute of Physics. [S0003-6951(98)04251-X]

As the dimension of Si microelectronic devices continue to decrease, it becomes increasingly important to understand how the point and extended defects evolve if shallow ion implanted junctions are to be realized. It has been known for several decades that ion implantation and subsequent annealing leads to the formation of dislocation loops which can lead to enhanced junction leakage.¹⁻³ These dislocation loops are extrinsic and are the result of "precipitation" of the excess interstitial population that exists after ion implantation. It is also known that rod-like {311} defects form upon annealing of self-implanted silicon. It has been shown that these {311} extended defects are a prime source of transient enhanced diffusion of dopants in silicon.⁴ How these defects evolve is the subject of great interest in the IC industry as they provide important clues on how to model junction depths after ion implantation and annealing.

The source of the dislocation loops has been the subject of speculation for many years. Wu and Washburn⁵ studied B-implanted Si by transmission electron microscopy (TEM). They observed that during annealing some small loops were growing up while the rod-shaped defects were dissolving. They suggested the dissolving rod-like defects were providing point defects for the growth of the extrinsic loops. Tan⁶ proposed a theoretical homogenous nucleation model for defect evolution. According to this model, energetically favorable condensation of point defects leads to formation of {311} defects and eventually dislocation loops, however, there was no experimental evidence to verify the model. Eaglesham *et al.*⁷ observed, by TEM, that several loops formed in a single row and suggested that the loops arise from the {311} defects unfauling. However, there was no direct confirmation that the unfauling of the {311} defect is the source of the dislocation loops. In this study, a series of micrographs were taken of the same region after *in situ* an-

nealing in order to follow the evolution of the {311} defects and dislocation loops. It is shown quantitatively that the unfauling of {311} defects is the source of the subthreshold dislocation loops.

Czochralski-grown (001) Si wafers were implanted at room temperature with Si⁺ ions at an energy of 100 keV and a dose of $2 \times 10^{14} \text{ cm}^{-2}$. This is below the amorphization threshold as confirmed by as-implanted cross-sectional TEM. After annealing at 800 °C for 5 min in a furnace, plan-view transmission electron microscopy (PTM) samples were made by mechanically grading the sample to $\sim 100 \mu\text{m}$, then etching with an HF:nitric acid=1:3 solution from the backside. Micrographs were taken after this preanneal and then the sample was annealed *in situ* at 800 °C using a Gatan heating holder on a JOEL 4000FX operating at 160 kV. The TEM images were taken under weak beam dark field g_{220} two-beam diffraction condition. The temperature was calibrated using two methods including a mounted thermocouple and the dissolution rate of the {311} defects.⁸ Comparison of the {311} dissolution rate with our measured values at different temperatures from conventional furnace annealing, indicates the temperature of the *in situ* furnace to be at 800 °C $\pm 5^\circ \text{C}$.⁸ These results also indicate there is not a measurable difference in dissolution rate between a sample annealed in a vacuum (*in situ*) and one annealed under flowing N₂ at this temperature.

Figure 1 shows the evolution of the {311} defects as a function of annealing time at 800 °C for samples annealed *in situ* in the TEM at 800 °C. The {311} defects are the rod-shaped defects while the loops are circular or elliptical. It is apparent from Fig. 1 that the {311} defects are dissolving and second that the dislocation loop density is increasing over the time interval between 5 and 40 min at 800 °C. In particular one {311} defect is shown by arrows to appear to be dissolv-

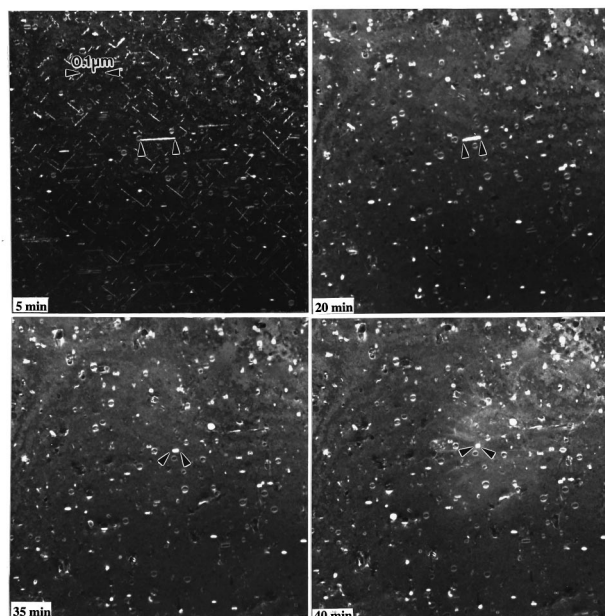


FIG. 1. Plan-view TEM images a 100 keV , $2 \times 10^{14}\text{ cm}^{-2}$ Si^+ -implanted Si sample after *in situ* annealing at $800\text{ }^\circ\text{C}$ for the noted times. The arrows show the unfaulting of a specific $\{311\}$ defect into a dislocation loop.

ing but in fact it has unfaulted into a loop. The results of the annealing can be quantified and is summarized graphically in Fig. 2. This graph shows how the density of $\{311\}$ defects and dislocation loops vary as a function of annealing time. It is apparent that when the $\{311\}$ defects are dissolving fastest the dislocation loops are forming fastest. This would suggest there is a correlation between the two events. It is also apparent from the graph that the loop density over the annealing times studied increased from 1×10^{11} to $2.5 \times 10^{11}/\text{cm}^2$ or an increase of $1.5 \times 10^{11}/\text{cm}^2$. Meanwhile, the $\{311\}$ density decreased from $3 \times 10^{11}/\text{cm}^2$ to less than $1 \times 10^9/\text{cm}^2$. The decrease in $\{311\}$ density is greater than the increase in

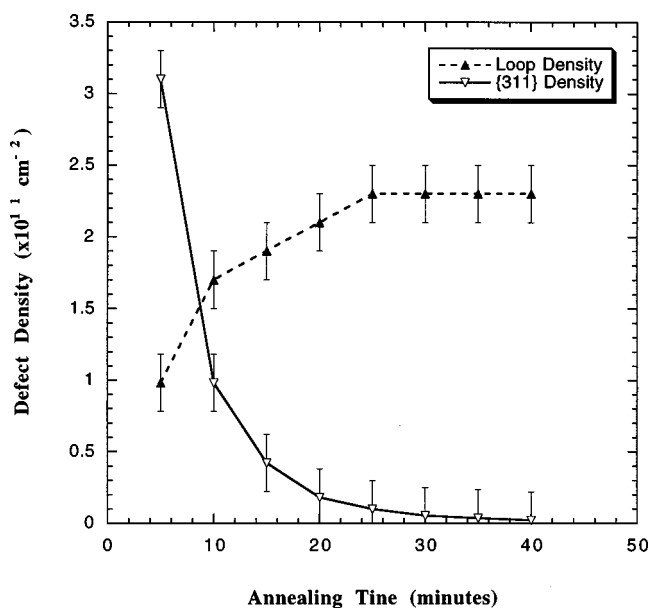


FIG. 2. Quantification of the TEM results for a 100 keV , $2 \times 10^{14}\text{ cm}^{-2}$ Si^+ implant after annealing at $800\text{ }^\circ\text{C}$. The graph shows both the $\{311\}$ density and dislocation loop density evolution as a function of *in situ* annealing time. The decay in the $\{311\}$ density corresponds to the growth in the loops.

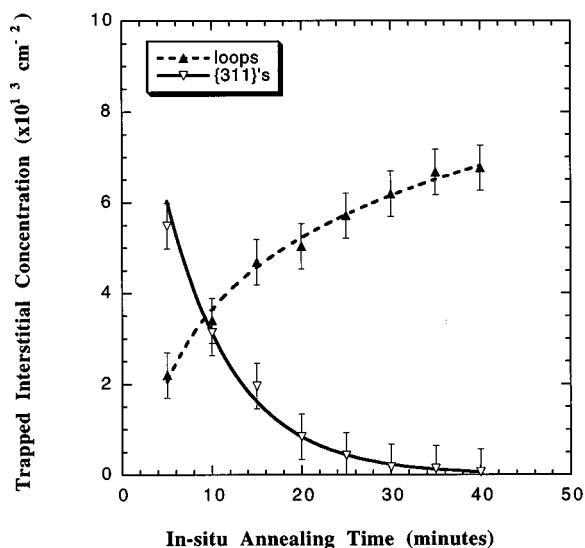


FIG. 3. Quantification of the TEM results for a 100 keV , $2 \times 10^{14}\text{ cm}^{-2}$ Si^+ implant after annealing at $800\text{ }^\circ\text{C}$. The graph shows the trapped interstitial concentration as a function of *in situ* annealing time. The decay in the interstitial in $\{311\}$ defects corresponds to the increase in interstitials in dislocation loops.

loop density. By dividing the dislocation loop density after 5 min by the final dislocation loop density (defined as when all of the $\{311\}$ defects have disappeared), it is apparent that 40% of the dislocation loops formed in the first 5 min of annealing.

To further study this process, the evolution of approximately 300 individual $\{311\}$ defects and 200 dislocation loops was followed on a defect by defect basis as a function of annealing time. From such studies, it was observed that every dislocation loops that formed over the annealing times studied (between 5 and 40 min) came from the unfaulting of a $\{311\}$ defect. This is the first quantitative evidence that the unfaulting of a $\{311\}$ defect is the source of a subthreshold dislocation loop.

If we now return to the density counts in Fig. 2, the density of $\{311\}$ defects dissolving was about $3 \times 10^{11}/\text{cm}^2$, while the density of loops forming was about $1.5 \times 10^{11}/\text{cm}^2$. Thus after $800\text{ }^\circ\text{C}$ annealing for 5 min, the probability of a $\{311\}$ defect eventually unfaulting into a loop was about 50%. It should be emphasized that these implants were nonamorphizing, therefore the conclusions apply only to loop formation at the projected range of nonamorphizing implants. The source of the loops in the end-of-range region for amorphizing implants may as well be the unfaulting of $\{311\}$ defects but this need to be verified. It is also clear from Fig. 2 that a substantial fraction (40%) of the total loop density forms in the first 5 min of annealing. Because every loop observed to form, after the first 5 min, was associated with a $\{311\}$ defect unfaulting, it is expected that this reaction may occur for shorter times as well. Future unfaulting studies at shorter times and lower temperatures will attempt to study the $\{311\}$ nucleation process as well as the loop formation process to ascertain the role of the unfaulting reaction in the formation of the loops formed in the first five minutes of annealing.

A quantitative analysis of the trapped interstitials in the defects is shown in Fig. 3. The quantification procedure for

both the $\{311\}$ defects and the dislocation loops has been reported previously.^{4,9-11} Figure 3 shows that approximately $6 \times 10^{13}/\text{cm}^2$ interstitial are trapped in $\{311\}$ defects and about $2 \times 10^{13}/\text{cm}^2$ interstitial are trapped in the loops after annealing at 800 °C for 5 min. Combined this is 40% of the implanted dose or a plus 0.4 dose of trapped interstitial.¹² Upon further annealing, the concentration of interstitials in the $\{311\}$ decreases as they unfault and dissolve. Meanwhile, the concentration in the loops increases because of the unfaulting and trapping of interstitials released by the $\{311\}$ defects. The increase in interstitial bound by loops is less than the dose in the $\{311\}$ defects, which means there is still net release of interstitials even when loops form. This is consistent with the observation that transient enhanced diffusion still occurs above the loop formation threshold for non-amorphizing implants. Over the course of the annealing times in this study (up to 800 °C 40 min) none of the dislocation loops were observed to dissolve. However, unpublished *in situ* studies have shown that with increasing time or temperature some loops will dissolve and they may well be an additional source of TED.

In order to study the unfaulting reaction further, a *g.b* analysis of the Burgers vectors of the dislocation loops was performed for a sample annealed at 800 °C for 30 min. It was determined that both faulted (Frank) loops with a Burgers vector of $a/3\langle 111 \rangle$ and perfect dislocation loops with a Burgers vector of $a/2\langle 110 \rangle$ were formed. Eaglesham *et al.*⁴ observed the formation of Frank loops after what appeared to be the unfaulting of a single $\{311\}$ defect for a 145 keV Si implant at a dose of $2 \times 10^{14}/\text{cm}^2$ and annealing at 900 °C for 15 min. Our analysis of ten defects indicated that 70% of the observed loops were Frank loops while $\sim 30\%$ were perfect loops. Determination of the Burgers vector of the $\{311\}$ defect has been the subject of several studies⁹ and best estimates indicate the vector is around $a/21\langle 116 \rangle$. This implies that the possible direct unfaulting reactions include for Frank loop formation:

$$a/21[116] + a/21[661] = a/3[111].$$

For the direct formation of a perfect loop, the reaction would be

$$a/21[116] + a/42[19, \bar{2}, 9] = a/2[101].$$

The energetics of the partial dislocation formation is such that the formation of the perfect loops is slightly less favorable than the formation of the Frank loop. This might help to explain the distribution of loop types.

In conclusion, the annealing kinetics of Si⁺-implanted Si have been investigated by *in situ* high temperature electron transmission microscopy. It has been shown quantitatively, that the unfaulting reaction of the $\{311\}$ defect is the source of the subthreshold dislocation loops that form after the first 5 min of annealing at 800 °C. These results imply there are two evolutionary paths the $\{311\}$ defects can follow upon annealing, dissolution, or unfaulting. The probability of a $\{311\}$ defect unfaulting after the first 5 min of annealing is around 50%. This suggests that for systems in which $\{311\}$ dissolution is the dominant source of transient enhanced diffusion (i.e., Si⁺ implants into Si), the competing reaction of dislocation loop formation by $\{311\}$ unfaulting would result in a saturation of TED with increasing dose.

The authors wish to thank Michael Wright and Kathryn Moller for preparing TEM samples. This research was supported by a grant from SEMATECH.

¹R. J. Schretelkamp, J. S. Custer, J. R. Liefing, W. X. Lu, and F. W. Saris, *Mater. Sci. Rep.* **6**, 275 (1991).

²J. R. Liefing, R. J. Schretelkamp, J. Vanhellefont, W. Vandervorst, K. Maex, J. S. Custer, and F. W. Saris, *Appl. Phys. Lett.* **63**, 1134 (1993).

³P. A. Stolk, H.-J. Gossmann, D. J. Eaglesham, D. C. Jacobson, C. J. Rafferty, G. H. Gilmer, M. Jaraiz, J. M. Poate, H. S. Luftman, and T. E. Haynes, *J. Appl. Phys.* **81**, 6031 (1997).

⁴D. J. Eaglesham, P. A. Stolk, H.-J. Gossmann, and J. M. Poate, *Appl. Phys. Lett.* **65**, 2305 (1994).

⁵W.-K. Wu and J. Washburn, *J. Appl. Phys.* **48**, 3744 (1977).

⁶T. Y. Tan, *Philos. Mag.* **44**, 101 (1981).

⁷D. J. Eaglesham, P. A. Stolk, H.-J. Gossmann, T. E. Haynes, and J. M. Poate, *Nucl. Instrum. Methods Phys. Res. B* **106**, 191 (1995).

⁸J.-H. Li, M. E. Law, C. Jasper, and K. S. Jones, *Materials Science in Semiconductor Processing* **8**, 1 (1998).

⁹I. G. Salisbury and M. H. Loretto, *Philos. Mag. A* **39**, 313 (1979).

¹⁰D. K. Sadana, M. Strathman, J. Washburn, and G. R. Booker, *J. Appl. Phys.* **52**, 774 (1981).

¹¹D. J. Eaglesham, A. Agarwal, T. E. Haynes, H.-J. Gossmann, D. L. Jacobson, and J. M. Poate, *Nucl. Instrum. Methods Phys. Res. B* **120**, 1 (1996).

¹²M. D. Giles, *J. Electrochem. Soc.* **138**, 1160 (1991).